Some Aspects of Space Fractional Quantum Mechanics

Bhabani Prasad Mandal
Banaras Hindu University, Varanasi, INDIA

PHHQP-XVIII
ICTS Bangalore
June 5, 2018

Preface

- Feynman path integral measure is generated by Brownian motion- Wiener stochastic process .
- This is basically Markov, Gaussian or normal stochastic process and statistical description is given by normal diffusion equation.
- Natural generalization of Brownian motion is the Levy flights, based on stable probability distribution, developed by Levy and follow generalized central limit theorem.
- Basically Levy flight is a random walk, in which the step lengths have a probability distribution with heavy tail.
- Levy flight paths are very useful to study Anomalous diffusion, Turbulence, Chaotic dynamics, fractals, financial dynamics etc and many others.

Preface

- Quantum mechanics formulated by replacing Brownian paths by Levy flight paths are known as Fractional Quantum Mechanics
- In this talk I will discuss some aspects of SFQM, Particularly based on our study on Hartman effect.
- The central theme of this conference is on Physics with Non-Hermitian operators , so naturally will consider Non-Hermitian extension of SFQM. Complex scattering has some typical characterestics, therefore I will discuss some scattering properties of NHSFQM.

Plan of the Talk

- Space Fractional Quantum Mechanics.
- Hartman Effect : SFQM
- Non-Hermitian SFQM
- Spectral Singularity in SFQM
- Coherent Perfect Absorption in SFQM
- Conclusions

Refs.

1. Tunneling in Space fractional Quantum Mechanics, M. Hasan & BPM, arXiv: 1712.08008 (PLA).
2. New Scattering features in NHSFQM, M Hasan & BPM, arXiv: 1712.09727

Feynman Path integral approach: The Kernal

$$K_F(x_b, t_b|x_a, t_a) = \int_{x_a}^{x_b} \mathcal{D}x(\tau)\ \exp\{\frac{i}{\hbar}\int_{t_a}^{t_b} d\tau V(x(\tau))\}$$

Where

$$\int_{x_a}^{x_b} \mathcal{D}\ x(\tau)\cdots =$$

$$\overset{Limit}{N \to \infty} \int \prod_{i=1}^{N-1} dx_i (\frac{m}{2\pi i\hbar\epsilon})^{\frac{N}{2}} \prod_{j=1}^{N} \exp\{\frac{im}{2\hbar\epsilon}(x_j - x_{j-1})^2\}\cdots$$

Levy approach (Fractional Quantum Mechanics)

$$\int_{x_a}^{x_b} \mathcal{D}\, x(\tau) \cdots$$

$$= N \overset{Limit}{\rightarrow} \infty \int \prod_{j=1}^{N-1} dx_j \left(\frac{\hbar}{iD_\alpha \epsilon}\right)^{\frac{N}{\alpha}} \prod_{j=1}^{N} L_\alpha \{ \left(\frac{\hbar}{iD_\alpha \epsilon}\right)^{1/\alpha} |x_j - x_{j-1}| \} \cdots$$

D_α is generalized diffusion coefficient , L_α is Levy function which is generally expressed as Fox 's H function and $1 < \alpha \leq 2$ is Levy index.

$\alpha = 2$

Levy distribution $\rightarrow$ Gaussian; Levy flight paths $\rightarrow$ Brownian paths.

Fractional Quantum Mechanics $\rightarrow$ Usual Quantum Mechanics.

Levy measure

In momentum representation,

$$\int_{x_a}^{x_b} \mathcal{D}\, x(\tau) \cdots$$

$$= N \overset{Limit}{\rightarrow} \infty \int \prod_{j=1}^{N-1} dx_j \frac{1}{(2\pi\hbar)^N} \int \prod_{j=1}^{N} dp_j \exp\{\sum_{j=1}^{N} [i \frac{p_j(x_j - x_{j-1})}{\hbar}$$

$$- i(\frac{D_\alpha \epsilon |p_j|^\alpha}{\hbar})]\} \cdots$$

with $x_0 = x_a$ and $x_N = x_b$.
The energy is given by $E_p = D_\alpha |p|^\alpha$
We are interested how Schrodinger eq. gets modified in SFQM
Ref: Laskin: PLA 268, 298 (2000)

Fractional Schrodinger Eq.

Fractional 1-d Schrodinger equation :

$$i\hbar\frac{\partial\psi(x,t)}{\partial t} = H_\alpha(x,t)\psi(x,t) \tag{1}$$

$H_\alpha(x,t)$ is the fractional Hamiltonian operator and is expressed through Riesz fractional derivative $(-\hbar^2\Delta)^{\alpha/2}$ as

$$\begin{aligned} H_\alpha(x,t) &= D_\alpha(-\hbar^2\Delta)^{\frac{\alpha}{2}} + V(x,t) \\ &= D_\alpha|p|^\alpha + V(x,t) \end{aligned} \tag{2}$$

$\Delta = \frac{\partial^2}{\partial x^2}$. The Riesz fractional derivative of the wave function $\psi(x,t)$ is defined through its Fourier transform $\tilde{\psi}(p,t)$ as

$$(-\hbar^2\Delta)^{\frac{\alpha}{2}}\psi(x,t) = \frac{1}{2\pi\hbar}\int_{-\infty}^{\infty}\tilde{\psi}(p,t)|p|^\alpha e^{\frac{ipx}{\hbar}}dp \tag{3}$$

Fractional Schrodinger Eq.

The Fourier transform of $\psi(x,t)$ is

$$\tilde{\psi}(p,t) = \int_{-\infty}^{\infty} \psi(x,t) e^{-i\frac{px}{\hbar}} dx \tag{4}$$

If potential $V(x,t)$ is independent of time we have the time independent fractional Hamiltonian operator $H_\alpha(x) = D_\alpha(-\hbar^2\Delta)^{\frac{\alpha}{2}} + V(x)$. In this case the time independent fractional Schrodinger equation is

$$D_\alpha(-\hbar^2\Delta)^{\frac{\alpha}{2}}\psi(x) + V(x)\psi(x) = E\psi(x) \tag{5}$$

where E is the energy of the particle and $\psi(x,t) = \psi(x)e^{-\frac{iEt}{\hbar}}$.

Fractional Quantum Mechanics

- Hermiticity: H_α is Hermitian, $< H_\alpha\phi|\psi >=< \phi|H_\alpha\psi >$ With the definition of Riesz fractional derivative, integration by parts formula $< \phi|(\hbar\nabla)^\alpha\psi >=< (\hbar\nabla)^\alpha\phi|\psi >$
- Parity Conservation:
  $PH_\alpha = H_\alpha P$ if $V(-x) = V(x)$ See, $e^{\frac{ipx}{\hbar}}$ is eigenfunction of Riesz fractional operator with eigenvalue $|p|^\alpha$
  $(\hbar\nabla_x)^\alpha \cdots = (\hbar\nabla_{-x})^\alpha \cdots$
- Continuity Eq.

$$\frac{\partial\rho}{\partial t} + \nabla \cdot J = 0$$

With $\rho = \psi^*\psi$ is the quantum mechanical probability density and probability current density $j = \frac{1}{\alpha}(\psi\hat{v}\psi^* + \psi^*\hat{v}\psi)$;
$\hat{v} = \alpha D_\alpha|\hat{p}^2|^{\alpha/2-1}\hat{p}$

Ref: Laskin (2010)

Tunnelling Time : SQM

To find the tunneling time τ consider the time evolution of a localized wave packet $G_{k_0}(k)$ given by normalized Gaussian function having peak at mean momentum $\hbar k_0$

$$\int G_{k_0}(k) e^{i(kx - \frac{Et}{\hbar})} dk \tag{6}$$

where wave number $k = \sqrt{2mE}$. The transmitted (through barrier) wave packet would be

$$\int G_{k_0}(k)|A(k)| e^{i(kx - \frac{Et}{\hbar} + \Phi(k))} dk \tag{7}$$

where $A(k) = |A(k)| e^{i\Phi(k)}$ is the transmission coefficient. In stationary phase method the tunnelling time τ is

$$\frac{d}{dk}\left(kb - \frac{E\tau}{\hbar} + \Phi(k)\right) = 0 \tag{8}$$

This gives the tunneling time expression as

$$\tau = \hbar \frac{d\Phi(E)}{dE} + \frac{b}{(\frac{\hbar k}{m})} \tag{9}$$

For a square barrier potential $V(x) = V$ confined over the region $0 \leq x \leq b$ and zero elsewhere, the tunnelling time is

$$\tau = \hbar \frac{d}{dE} \tan^{-1} \left(\frac{k^2 - q^2}{2kq} \tanh qb \right) \tag{10}$$

In the above equation, $q = \sqrt{2m(V-E)}/\hbar$. Observe that $\tau \to 0$ as $b \to 0$ as expected, however when $b \to \infty$, $\tau = \frac{2m}{\hbar q k}$, i.e. tunneling time is independent of the width of the barrier b for sufficiently opaque barrier. Using units $2m = 1$, $\hbar = 1$, $c = 1$

$$\lim_{b \to \infty} \tau = \frac{1}{qk} \tag{11}$$

The tunnelling time is independent of the width of the barrier for sufficiently thick barrier.

HF: SQM

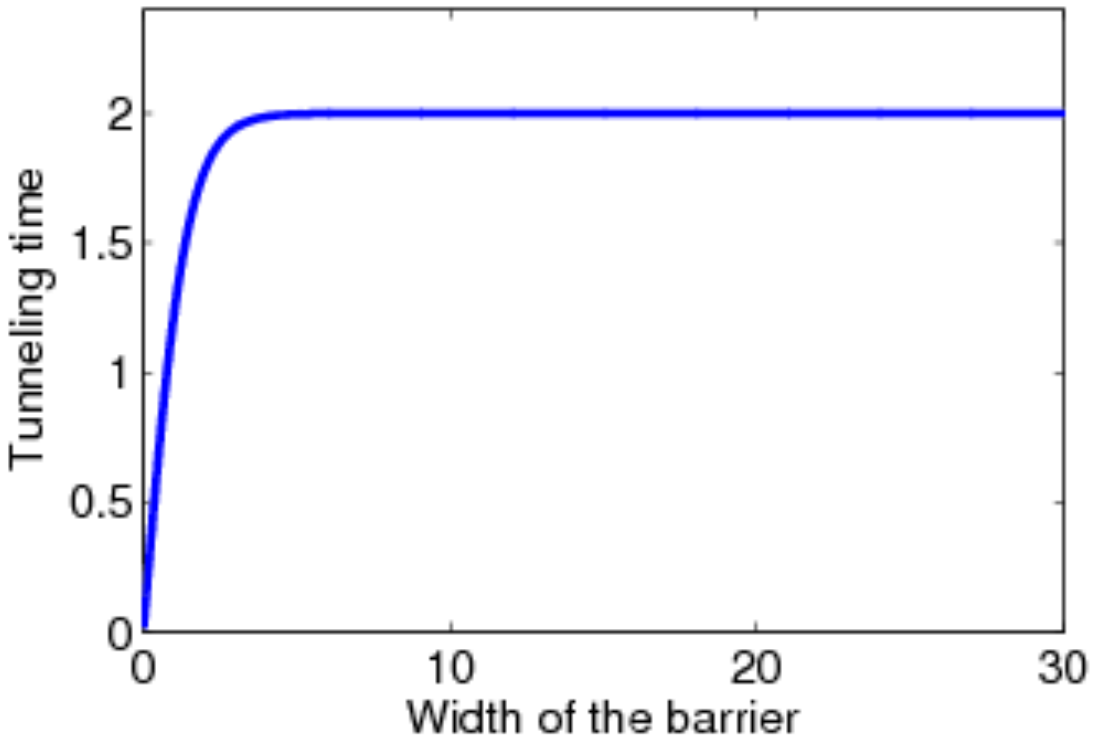

Hartman Effect: Complex potentials

- Hartman effect has also been studied for single complex barrier, i.e. in presence of absorption. Ref: B. Dutta Roy etal (2007)
- For series of complex barrier, saturation is obtained w. r. t for number of barriers for low absorption, i.e. for small V_c coupling between elastic and non-elastic channels.
- Tunnelling time has typical characteristics and saturation is obtained under different conditions.

Square barrier potential

$$V(x) = V, \qquad 0 \leq x \leq b \text{ and } V = 0 \text{ elsewhere} \tag{12}$$

The TISFSE is

$$D_\alpha(-\hbar^2\Delta)^{\frac{\alpha}{2}}\psi(x) + V\psi(x) = E\psi(x) \tag{13}$$

The general solutions

$$\psi(x) = \begin{cases} Ae^{ik_\alpha x} + Be^{-ik_\alpha x}, & x < 0 \\ C\cos\overline{k}_\alpha x + D\sin\overline{k}_\alpha x, & 0 < x < b \\ Fe^{ik_\alpha x} + Ge^{-ik_\alpha x}, & x > b \end{cases} \tag{14}$$

where,

$$\begin{aligned} k_\alpha &= \left(\frac{E}{D_\alpha\hbar^\alpha}\right)^{\frac{1}{\alpha}} \\ \overline{k}_\alpha &= \left(\frac{E-V}{D_\alpha\hbar^\alpha}\right)^{\frac{1}{\alpha}} \end{aligned} \tag{15}$$

SFQM:Transmission Coefficient

The transmission coefficient,

$$\overline{t} = \frac{e^{-ik_\alpha b}}{\cos \overline{k}_\alpha b - i\mu \sin \overline{k}_\alpha b} \tag{16}$$

where,

$$\mu = \frac{1}{2}\left(\varepsilon + \frac{1}{\varepsilon}\right); \qquad \varepsilon = \left(\frac{k_\alpha}{\overline{k}_\alpha}\right)^{\alpha-1} \tag{17}$$

For classically forbidden case, $E < V$, transmission coefficient is

$$\overline{t} = \frac{e^{-ik_\alpha b}}{\cos k'_\alpha b - i\mu \sin k'_\alpha b} \tag{18}$$

where,

$$k'_\alpha = (-1)^{\frac{1}{\alpha}} \left(\frac{V-E}{D_\alpha}\right)^{\frac{1}{\alpha}} = q_\alpha e^{i\frac{\pi}{\alpha}} \tag{19}$$

and,

$$q_\alpha = \left(\frac{V-E}{D_\alpha}\right)^{\frac{1}{\alpha}} \tag{20}$$

Phase:Transmission Coefficient

The phase in $\bar{t}$ is obtained as

$$\Phi = \theta - k_\alpha b \tag{21}$$

where

$$\theta = \tan^{-1}\frac{Y}{X} \quad \text{and} \quad \cos k'_\alpha b - i\mu \sin k'_\alpha b = X - iY \tag{22}$$

To find the phase delay time we evaluate $\frac{d\theta}{dE}$.

$$\frac{d\theta}{dE} = \frac{d_\alpha}{(\cos^2 k'_\alpha b + \mu^2 \sin^2 k'_\alpha b)} \tag{23}$$

$$d_\alpha = \left(X\frac{dY}{dE} - Y\frac{dX}{dE}\right) \tag{24}$$

Phase:Transmission Coefficient

$$
\begin{aligned}
d_\alpha = {} & \frac{1}{2} b\varepsilon_+ q'_\alpha \cos\beta \cos\gamma \cosh 2\xi + \frac{1}{2} b\varepsilon_- q'_\alpha \sin\beta \sin\gamma \cos 2\eta \\
& + \frac{1}{4}\varepsilon'_+ \cos\beta \sin 2\eta - \frac{1}{2} b q'_\alpha (\sin\gamma \sin 2\eta + \cos\gamma \sinh 2\xi) \\
& + \frac{1}{8} b q'_\alpha (\sin 2\eta \sin\gamma - \sinh 2\xi \cos\gamma)(\varepsilon_+^2 \cos^2\beta + \varepsilon_-^2 \sin^2\beta) \\
& + \frac{1}{8} \sin 2\beta (\cosh^2 2\xi \sin^2\eta + \sinh^2 2\xi \cos^2\eta)(\varepsilon_-\varepsilon'_+ - \varepsilon_+\varepsilon'_-) \\
& + \frac{1}{4}\varepsilon'_- \sin\beta \sinh 2\xi \qquad (25)
\end{aligned}
$$

The denominator of Eq. 23 is

$$v_\alpha = \cos^2 k'_\alpha b + \mu^2 \sin^2 k'_\alpha b = \frac{1}{16}\Big[\{8 - \varepsilon_-^2 - \varepsilon_+^2 - (\varepsilon_+^2 - \varepsilon_-^2)\cos 2\beta\}\cos 2\eta + \{8 + \varepsilon_-^2 + \varepsilon_+^2 + (\varepsilon_+^2 - \varepsilon_-^2)\cos 2\beta\}\cosh 2\xi + 8\varepsilon_- \sin\beta \sin 2\eta - 8\varepsilon_+ \cos\beta \sinh 2\xi\Big] \quad (26)$$

Here,

$$\eta = q_\alpha b \cos\frac{\pi}{\alpha}, \quad \xi = q_\alpha b \sin\frac{\pi}{\alpha}, \quad \beta = \frac{\alpha - 1}{\alpha}\pi, \quad \gamma = \frac{\pi}{\alpha} \quad (27)$$

and,

$$q'_\alpha = \frac{dq_\alpha}{dE} = -\frac{1}{\alpha D_\alpha} q_\alpha^{1-\alpha} \quad (28)$$

Tunnelling Time

$$\varepsilon_{\pm} = \varepsilon_{\alpha} \pm \frac{1}{\varepsilon_{\alpha}} \tag{29}$$

$$\varepsilon'_{\pm} = \frac{d\varepsilon_{+}}{dE} = \frac{\alpha - 1}{\alpha} \frac{V}{(V-E)^2} \varepsilon_{\alpha}^{\frac{1}{1-\alpha}} (1 \mp \varepsilon_{\alpha}^{-2}) \tag{30}$$

Also,

$$\frac{dk_{\alpha}}{dE} = \frac{k_{\alpha}^{1-\alpha}}{\alpha D_{\alpha}} \tag{31}$$

Therefore the tunneling time from a rectangular barrier in space fractional quantum mechanics is given by

$$\tau_{\alpha} = \hbar \left(\frac{d_{\alpha}}{v_{\alpha}} - \frac{b k_{\alpha}^{1-\alpha}}{\alpha D_{\alpha}} \right) + \frac{b}{\frac{\hbar k}{m}} \tag{32}$$

Where d_{α} and v_{α} are obtained from Eqs. 25 and 26 respectively.

Tunnelling Time

for large b, the tunneling time expression (eq. 32) becomes

$$\lim_{b\to\infty} \tau_\alpha = b\left(q'_\alpha \tau_{1\alpha} - \frac{k_\alpha^{1-\alpha}}{\alpha D_\alpha} + \frac{1}{2k}\right) + \tau_{2\alpha} \tag{33}$$

This linearly depends on the width of the barrier b.

$$\tau_{1\alpha} = \frac{\cos\gamma\left[(\varepsilon_+\cos\beta - 1) - \frac{1}{4}(\varepsilon_+^2\cos\beta^2 + \varepsilon_-^2\sin\beta^2)\right]}{1 + \frac{1}{8}[\varepsilon_+^2 + \varepsilon_-^2 + (\varepsilon_+^2 - \varepsilon_-^2)\cos 2\beta] - \varepsilon_+\cos\beta} \tag{34}$$

$$\tau_{2\alpha} = \frac{\frac{1}{4}\sin 2\beta(\varepsilon_-\varepsilon'_+ - \varepsilon'_-\varepsilon_+) + \frac{1}{2}\varepsilon'_-\sin\beta}{1 + \frac{1}{8}[\varepsilon_+^2 + \varepsilon_-^2 + (\varepsilon_+^2 - \varepsilon_-^2)\cos 2\beta] - \varepsilon_+\cos\beta} \tag{35}$$

No Hartman Effect in SFQM

No HF effect

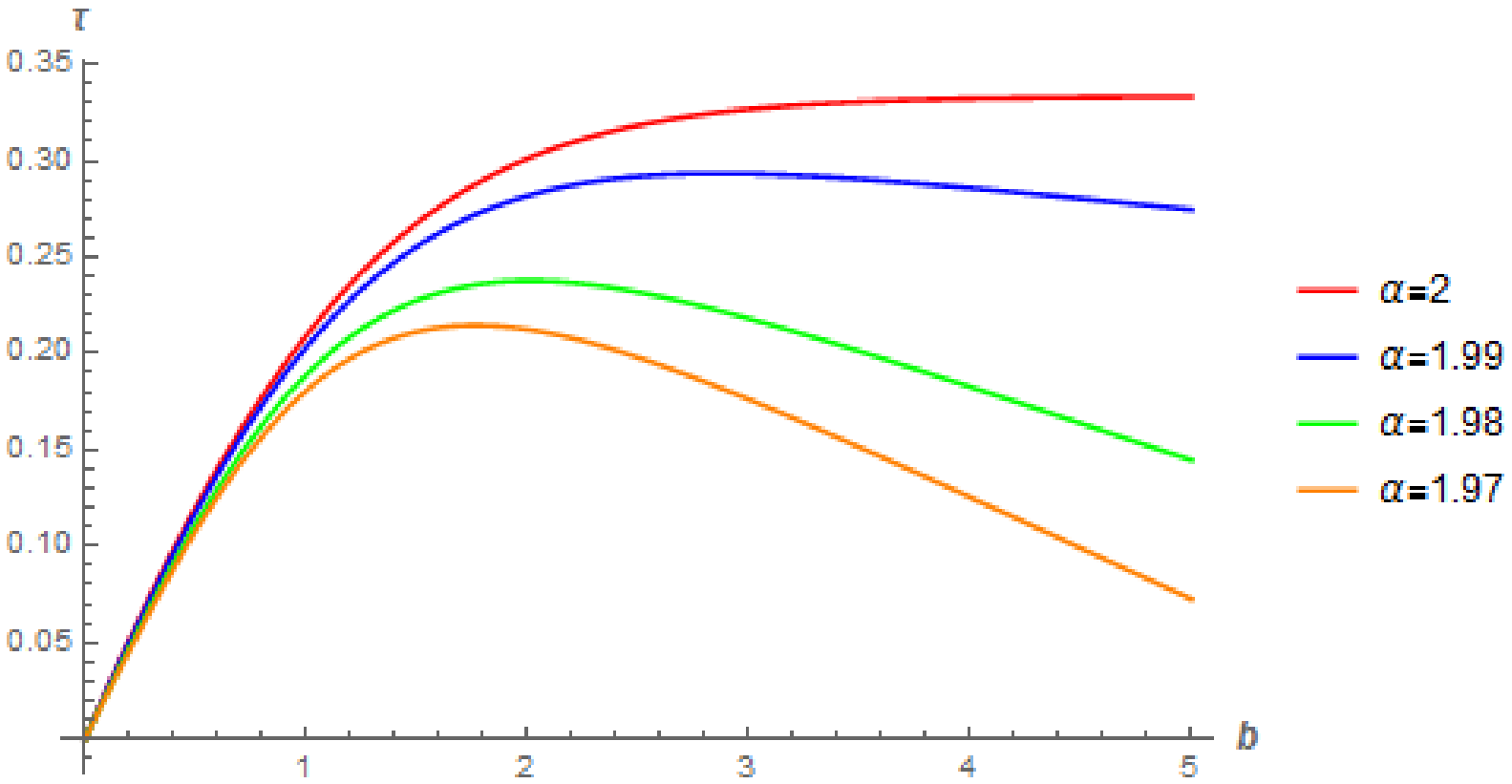

Figure: Tunneling time τ VS width 'b' for different α values. $V = 10$, $E = 9$ and $u = 10^{-4}c$, $c = 1$.

HF is recovered in SQM limit

For $\alpha = 2$ we have $\beta = \frac{\pi}{2}$ and $\gamma = \frac{\pi}{2}$. With these values, $\tau_{1\alpha} = 0$. Thus

$$k = k_2 = \sqrt{E}$$

$$q = q_2 = \sqrt{E - V}$$

We take the generalized diffusion coefficient D_α as

$$D_\alpha = \frac{u^{2-\alpha}}{\alpha m^{\alpha-1}} \tag{36}$$

where u is the characteristic velocity of the non-relativistic system. Therefore in the chosen unit

$$D_2 = 1$$

Substitution these in tunneling time

$$\lim_{b\to\infty} \tau_2 = \tau_{2\alpha}(\alpha = 2) \tag{37}$$

Ref: Hasan & Mandal, PLA (2018)

Non-Hermitian Space Fractional Quantum Mechanics

Transfer Matrix :NHSFQM

Consider the complex delta potential

$$V(x) = \zeta\delta(x - x_0) \tag{38}$$

ζ is a complex number. The transfer matrix

$$M = \begin{pmatrix} m_{11} & m_{12} \\ m_{21} & m_{22} \end{pmatrix} \tag{39}$$

In SFQM,

$$m_{11} = 1 + i\zeta(2D_\alpha k_\alpha^{\alpha-1}\hbar^\alpha)^{-1} \tag{40}$$

$$m_{22} = 1 - i\zeta(2D_\alpha k_\alpha^{\alpha-1}\hbar^\alpha)^{-1} \tag{41}$$

$$m_{12} = i\zeta(2D_\alpha k_\alpha^{\alpha-1}\hbar^\alpha)^{-1} \tag{42}$$

$$m_{21} = -i\zeta(2D_\alpha k_\alpha^{\alpha-1}\hbar^\alpha)^{-1} \tag{43}$$

$$k_\alpha = \left(\frac{E}{D_\alpha\hbar^\alpha}\right)^{\frac{1}{\alpha}} \tag{44}$$

NHSFQM: $\delta-$ potential

At $E = E_{ss}$, $E_{ss} \in R^+$, We have spectral singularity if $m_{22}(E_{ss}) = 0$.
Need to solve

$$1 - i\zeta(2D_\alpha k_\alpha^{\alpha-1}\hbar^\alpha)^{-1} = 0 \tag{45}$$

The solution ($\hbar = 1$, $m = 1$, $v = 1$) with $\zeta = |\zeta|e^{i\phi}$

$$E_{ss} = \left(\frac{1}{D_\alpha}\right)^{\frac{1}{\alpha-1}} \left(\frac{|\zeta|}{2}\right)^{\frac{\alpha}{\alpha-1}} e^{\frac{i\alpha}{\alpha-1}\left(\frac{\pi}{2}+\phi\right)} \tag{46}$$

For real E, $\phi = -\frac{\pi}{2}$. Hence $\zeta = -i\rho$, $\rho \in R^+$ and $D_\alpha = \frac{1}{\alpha}$.

NHSFQM δ-potential: SS

The delta potential $V(x) = -i\rho\delta(x - x_0)$, $(\rho \in R^+)$ admits spectral singularity at,

$$E_{ss}^{\alpha} = \alpha^{\frac{1}{\alpha-1}} \left(\frac{\rho}{2}\right)^{\frac{\alpha}{\alpha-1}} \tag{47}$$

For a given α, E_{ss} increases with ρ. Further, we compare this SS SQM

$$\frac{E_{ss}^{\alpha}}{E_{ss}} = \left(\frac{\alpha^{\frac{1}{\alpha-1}}}{2}\right)\left(\frac{2}{\rho}\right)^{\frac{\alpha-2}{(\alpha-1)}} \equiv f(\alpha, \rho) \tag{48}$$

The term $\frac{1}{2}(\alpha^{\frac{1}{\alpha-1}})$ is greater than unity for the range $1 < \alpha \leq 2$. Therefore if $\rho > 2$ then we always have $E_{ss}^{\alpha} \geq E_{ss}$ for $1 < \alpha \leq 2$. That is SS is blue shifted. Also note:

$$\lim_{\alpha \to 1^+} \left(\frac{2}{\rho}\right)^{\frac{\alpha-2}{(\alpha-1)}} \to \infty \quad \text{, for } \rho > 2 \tag{49}$$

NHSFQM δ-potential: SS

- SS energy is blue shifted with decreasing α for $\rho > 2$ and the upper bound on $f(\alpha, \rho)$ is ∞.
- If $\rho > 2$, then one can have SS at any energy $E > E_{ss}$ in non-Hermitian SFQM with a suitably chosen Levy index α.
- According to the limiting case given by Eq. 49 all curve for $\rho > 2$ must diverge for $\alpha \to 1^{+}$.

Blue shifted SS

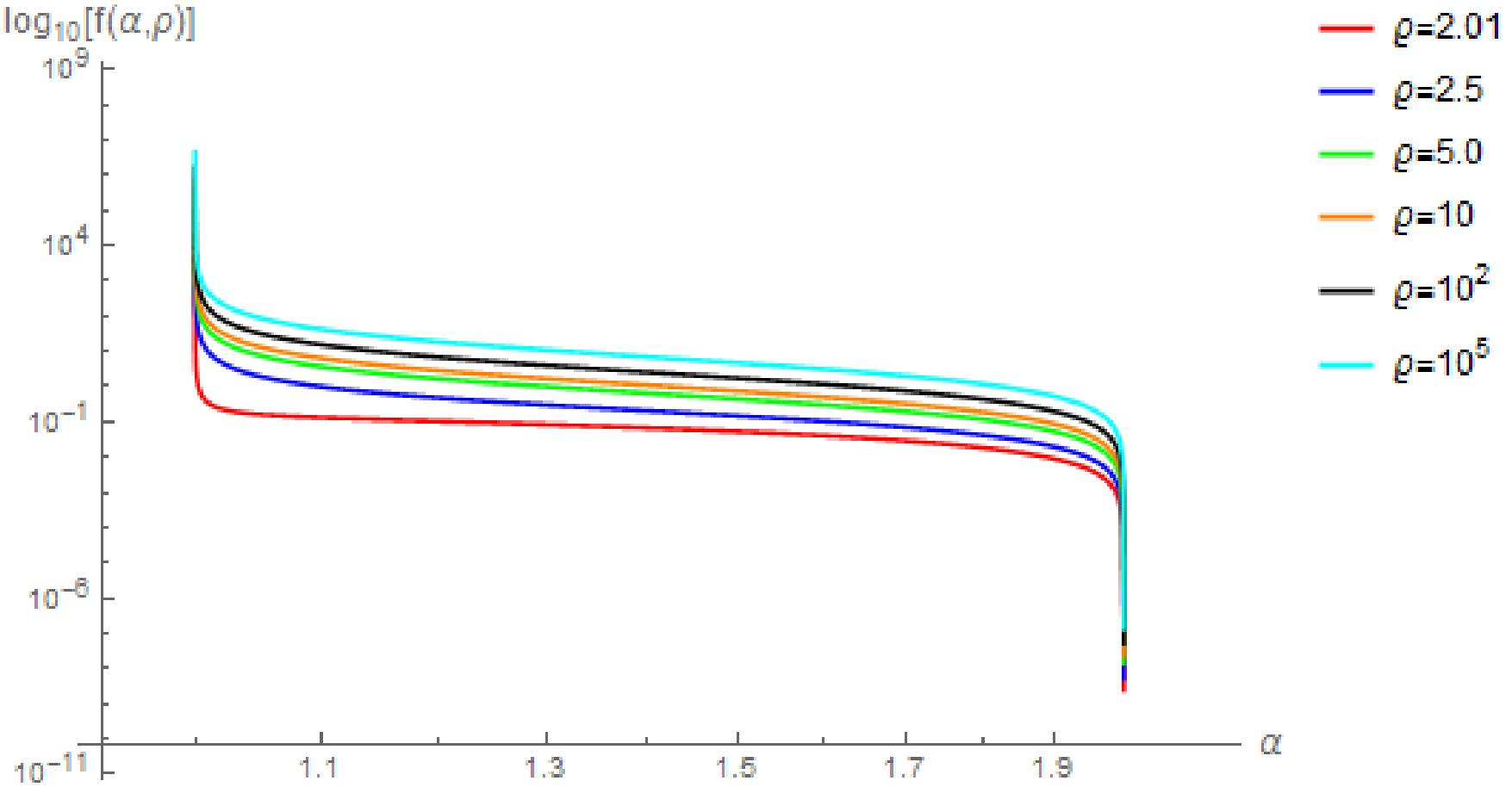

Figure: *log-log plot of* $\log_{10} f(\alpha, \rho)$ *for the delta potential* $V(x) = -i\rho\delta(x - x_0)$ *for different values of* $\rho > 2$ *with* α. *The SS energy is blue shifted as compared to SS energy when* $\alpha = 2$.

Red Shifted

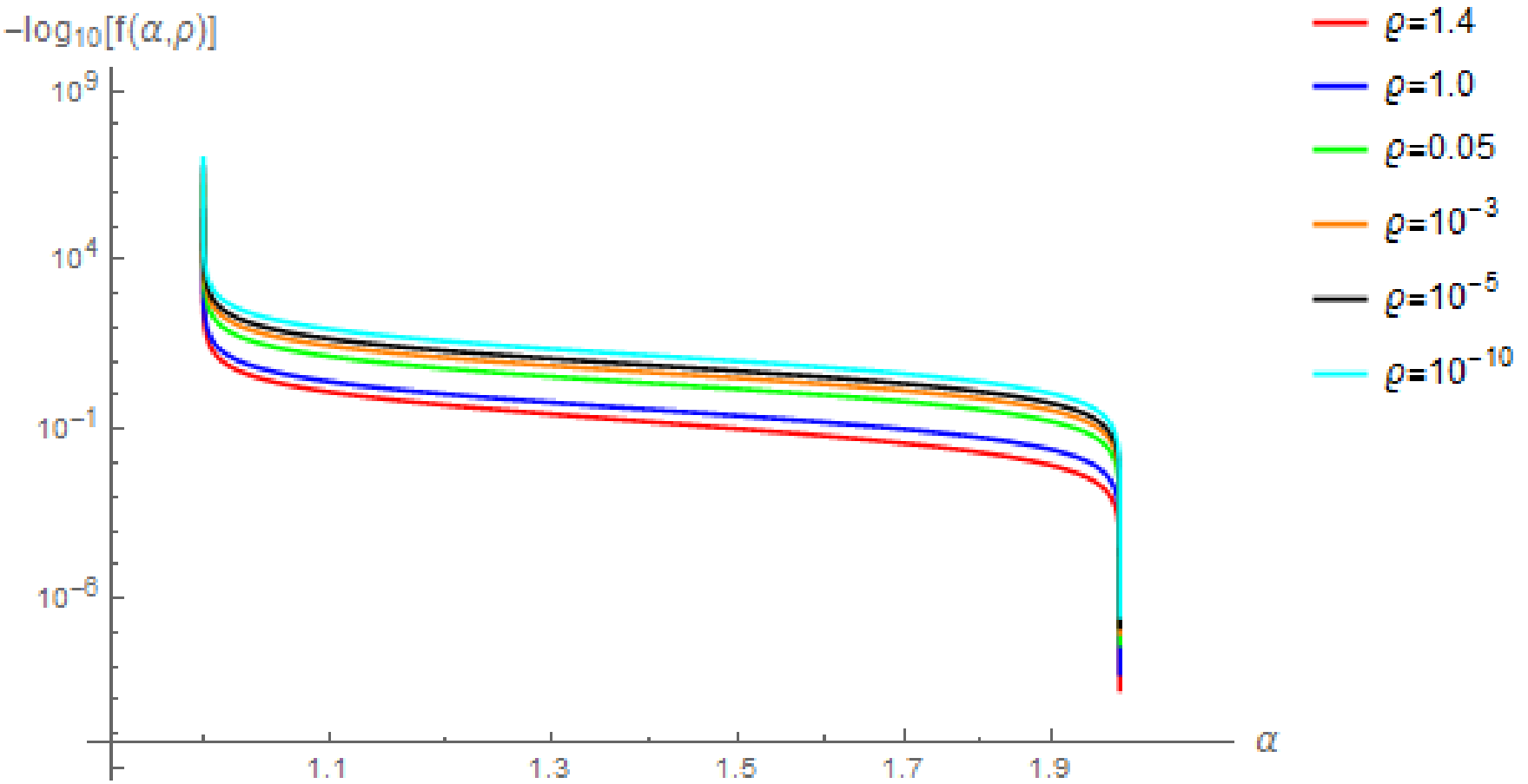

Figure: *log-log plot of* $-\log_{10} f(\alpha, \rho)$ *for the delta potential* $V(x) = -i\rho\delta(x - x_0)$ *for different values of* $0 < \rho < \frac{4}{e}$ *with* α. *The SS energy is red shifted as compared to SS energy when* $\alpha = 2$.

Blue shifted SS

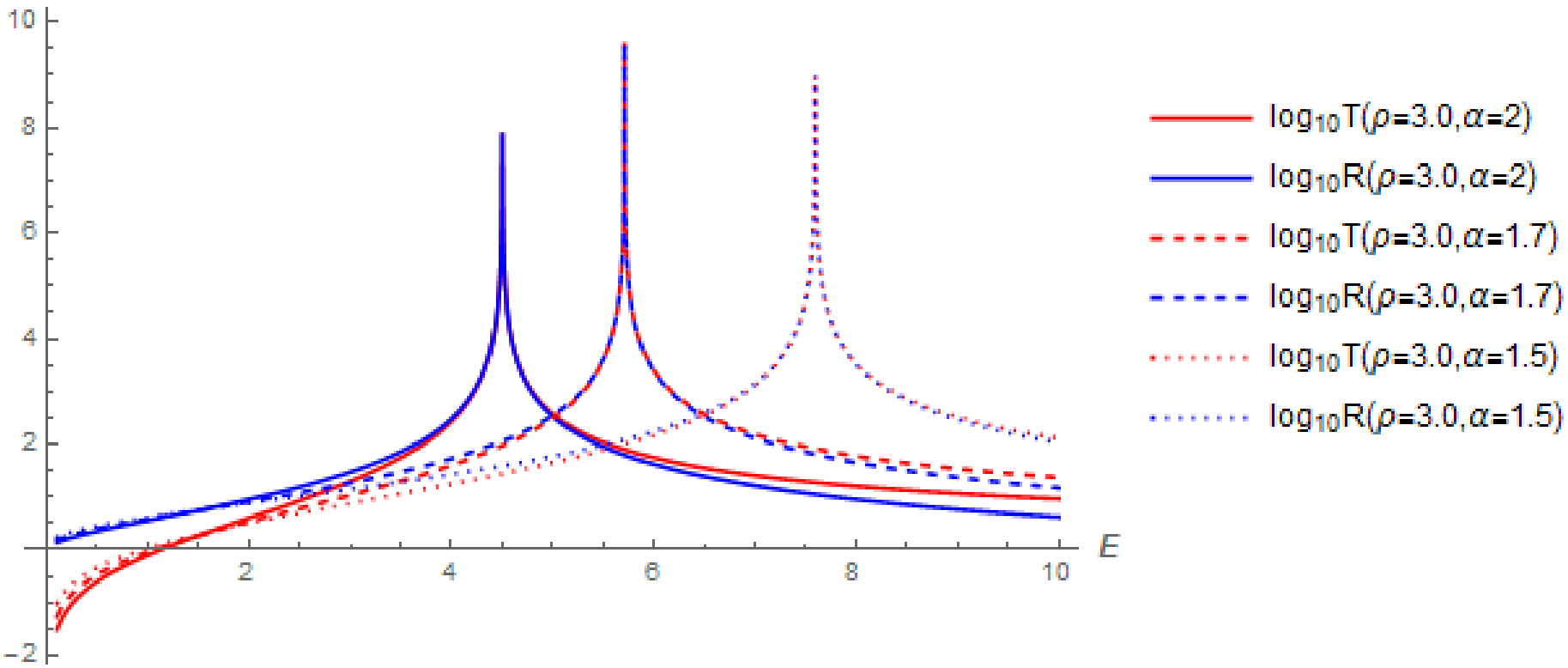

Figure: *The spectral singularity for the delta potential* $V(x) = -3i\delta(x - x_0)$ *for different values of* α*. The SS energy is blue shifted as* α *decreases when* $\rho > 2$

Red Shifted SS

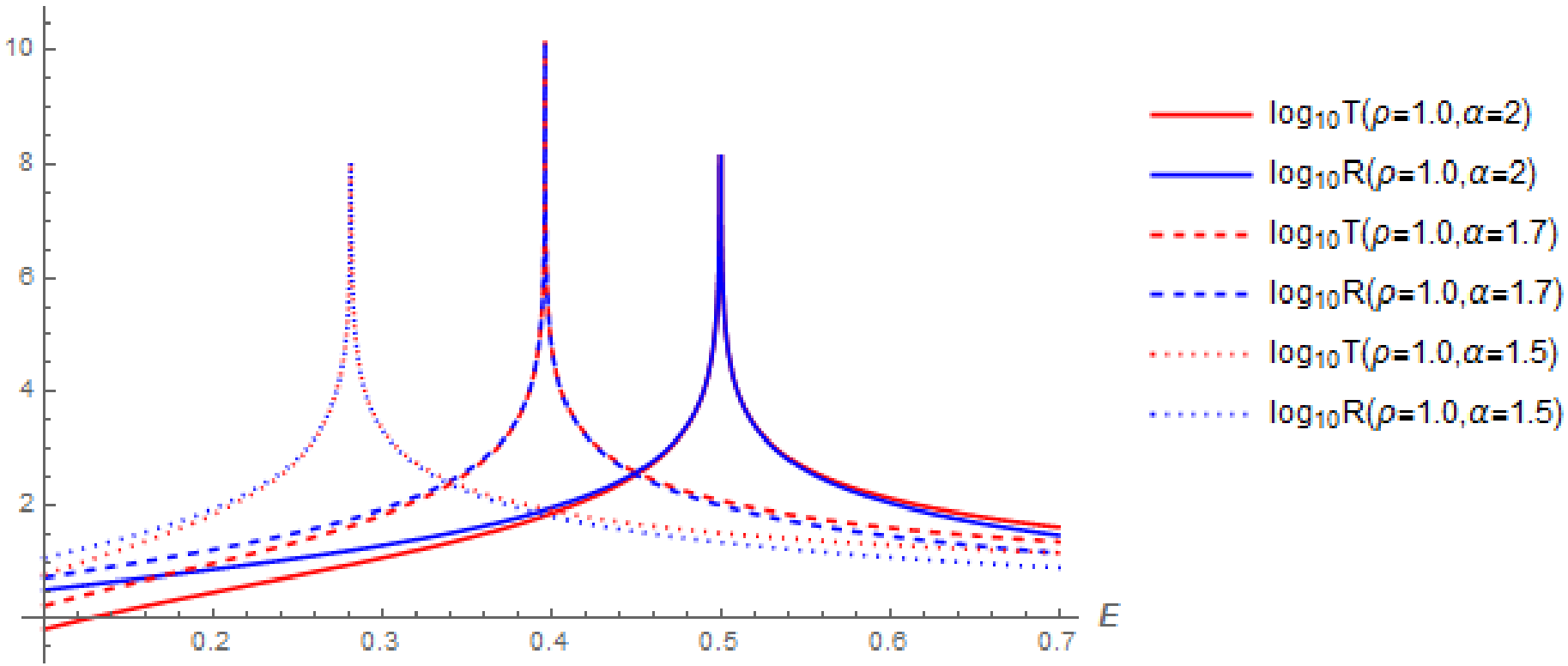

Figure: *The spectral singularity for the delta potential* $V(x) = -i\delta(x - x_0)$ *for different values of* α*. The SS energy is red shifted as* α *decreases when* $\rho < \frac{4}{e}$.

NHSFQM: Barrier Potential

$V(x) = V = V_1 + iV_2$, $\{V_1, V_2\} \in R$ over the interval $(0, b)$ and zero elsewhere.
The transfer matrix in SFQM

$$\begin{aligned} m_{11} &= (\cos \overline{k}_\alpha b - i\mu_1 \sin \overline{k}_\alpha b) e^{ik_\alpha b} \\ m_{22} &= (\cos \overline{k}_\alpha b + i\mu_1 \sin \overline{k}_\alpha b) e^{-ik_\alpha b} \\ m_{12} &= i\mu_2 \sin \overline{k}_\alpha b \\ m_{21} &= -i\mu_2 \sin \overline{k}_\alpha b \end{aligned} \tag{50}$$

where,

$$\mu_1 = \frac{1}{2}\left(\varepsilon + \frac{1}{\varepsilon}\right) \tag{51}$$

$$\mu_2 = \frac{1}{2}\left(\varepsilon - \frac{1}{\varepsilon}\right) \tag{52}$$

Complex Barrier

$$\varepsilon = \left(\frac{k_\alpha}{\overline{k}_\alpha}\right)^{\alpha-1} \tag{53}$$

$$\overline{k}_\alpha = \left(\frac{E-V}{D_\alpha \hbar^\alpha}\right)^{\frac{1}{\alpha}} \tag{54}$$

The reflection and transmission amplitudes are obtained as

$$t_l = \frac{1}{m_{22}} \quad , r_l = \frac{m_{21}}{m_{22}} \tag{55}$$

$$t_r = \frac{1}{m_{22}} \quad , r_r = \frac{m_{12}}{m_{22}} \tag{56}$$

SS and CPA

- The corresponding coefficients are $T_{l,r} = |t_l = t_r|^2$, $R_{l,r} = |r_{l,r}|^2$.
- The SS corresponds to the simultaneous blow up of of $T_{l,r}$ and $R_{r,l}$ at a particular real energy for unidirectional incidence. i.e. $E = E_{ss}$, $E_{ss} \in R^+$, one has the SS if $m_{22}(E_{ss}) = 0$ i.e. the real energy at which the zeros of m_{22} occur.
- The condition for CPA

$$t_l(E)t_r(E) - r_l(E)r_r(E) = 0 \tag{57}$$

for $E = E_{CPA} \in R^+$.

SS: Complex Barrier

- At $E_{ss} \in R^+$, the spectral singularity is given by the relation

$$\cos \overline{k}_\alpha b + i\mu_1 \sin \overline{k}_\alpha b = 0 \tag{58}$$

- This transcendental equation has been solved for non-Hermitian potential barrier by analytical method in SQM. But difficult to solve for SFQM.
- We numerically find spectral singularity considering the variation of R_l and T_l. SS for different values of α is shown graphically.
- As α decreases, the divergence in R and T i.e. SS is blue shifted.

Blue shifted SS for complex barrier

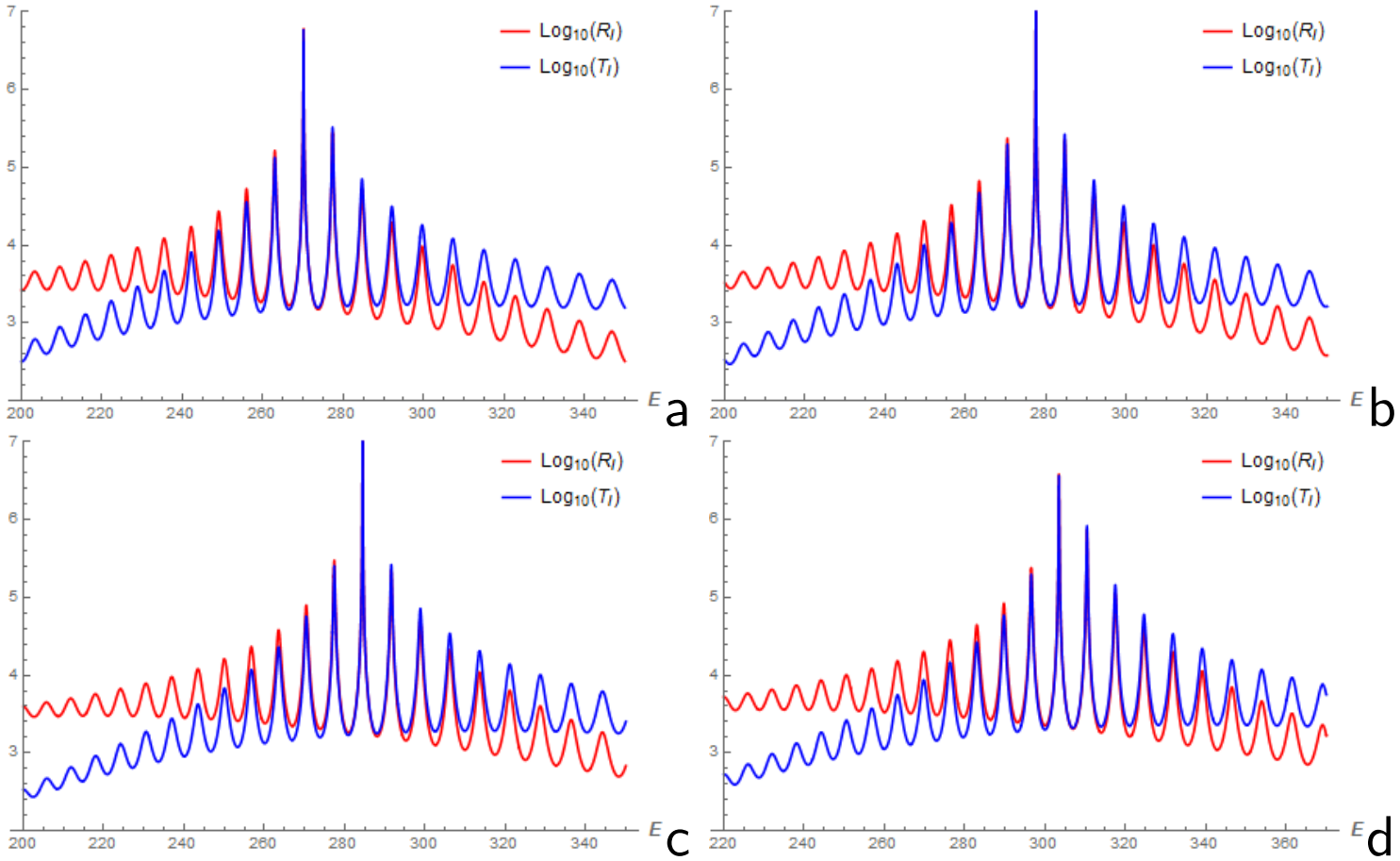

Figure: *The SS for* $V = 9.1675 - 10i$ *of width* $b = 10$ *for different values of* α*. The red and blue curves represent* $\log_{10} R_l$ *and* $\log_{10} T_l$ *respectively. For the figure a, b, c and d the values of* α *are* 2, 1.99, 1.98 *and* 1.95 *respectively. The SS energy is blue shifted as* α *decreases.*

Sub Peaks

- Sub-Peaks
  We observe that to the both sides of the simultaneous peak (and the maxima) in $\log_{10} R$ and $\log_{10} T$ for $\alpha = 2$ there are relatively small peaks in $\log_{10} R$ and $\log_{10} T$ due to their oscillations with E for $E > E_{ss}^{\alpha=2}$ and $E < E_{ss}^{\alpha=2}$. We will call these peaks in $\log_{10} R$ and $\log_{10} T$ around $E_{ss}^{\alpha=2}$ as '*sub-peaks*' around $E_{ss}^{\alpha=2}$.
- We observe that the sub-peaks for $E > E_{ss}^{\alpha=2}$ grow in amplitude as α decreases till the simultaneous maxima (and the top maxima) in R and T appear. This has been demonstrated graphically
- Again it is evident from the figures that each sub-peak for $E > E_{ss}^{\alpha=2}$ of non-Hermitian SQM develops a simultaneous maxima in R and T for some values of $\alpha < 2$ in non-Hermitian SFQM.

SS at different values

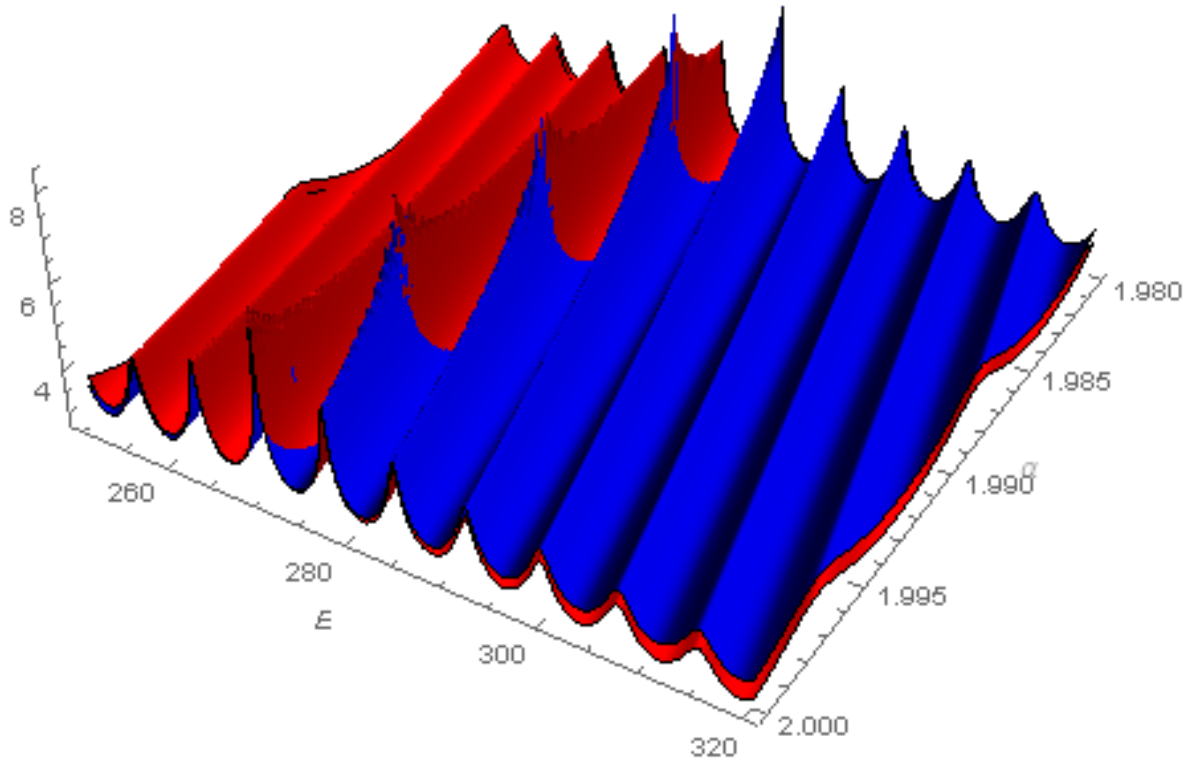

a

Figure: *SS for* $\alpha \leq 2$ *in* $\alpha - E$ *space. Red and blue plots represent* $\log_{10} R$ *and* $\log_{10} T$ *. The range of* α *is* $1.98 \leq \alpha \leq 2$ *The peak of the oscillations in* $\log_{10} R$, $\log_{10} T$ *for* $\alpha = 2$ *and* $E > E_{ss}^{\alpha=2}$ *slowly amplify with decreasing* α *and develop SS f* $\alpha < 2$.

SS at different values

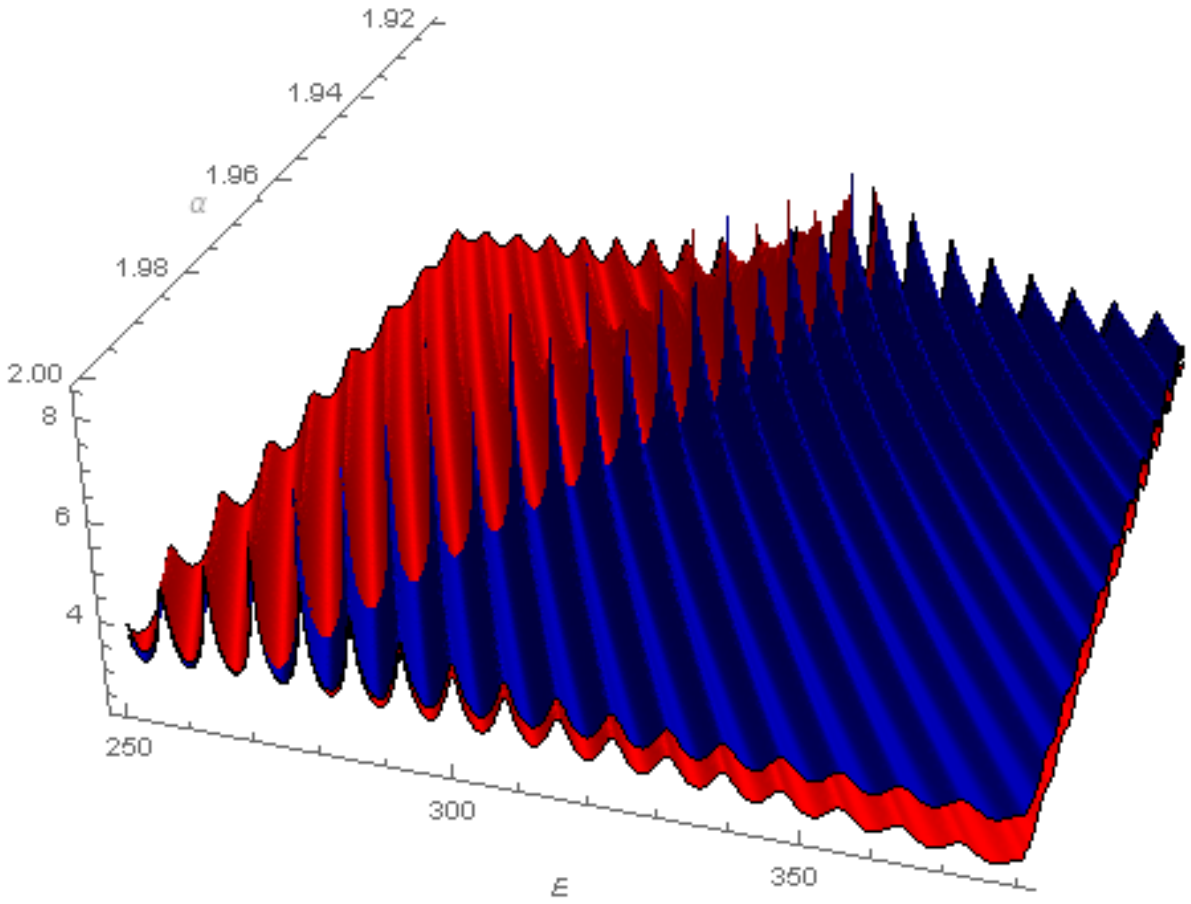

b

Figure: *SS for* $\alpha \leq 2$ *in* $\alpha - E$ *space. Red and blue plots represent* $\log_{10} R$ *and* $\log_{10} T$ $1.92 \leq \alpha \leq 2$. *The peak of the oscillations in* $\log_{10} R$, $\log_{10} T$ *for* $\alpha = 2$ *and* $E > E_{ss}^{\alpha=2}$ *slowly amplify with decreasing* α *and develop SS for* $\alpha < 2$.

SS at different values

- This is a new features of scattering in non-Hermitian SFQM and shows that non-Hermitian SFQM is more flexible for spectral singularity. A closer look of the development of SS from the first sub-peak is shown below graphically
- For $E > E_{ss}^{\alpha=2}$ sub-peaks develop as SS in the decreasing order of α values ($\alpha < 2$) in non-Hermitian SFQM. This explains the blue shift of SS energy in non-Hermitian SFQM with reducing α.
- Similarly we have checked that the sub-peaks occurring for $E < E_{ss}^{\alpha=2}$, develop SS for $\alpha > 2$. However as the range of α is limited to $1 < \alpha \leq 2$ in SFQM, therefore we are not discussing the case of $\alpha > 2$.

Close view for 1st Sub-Peak to SS

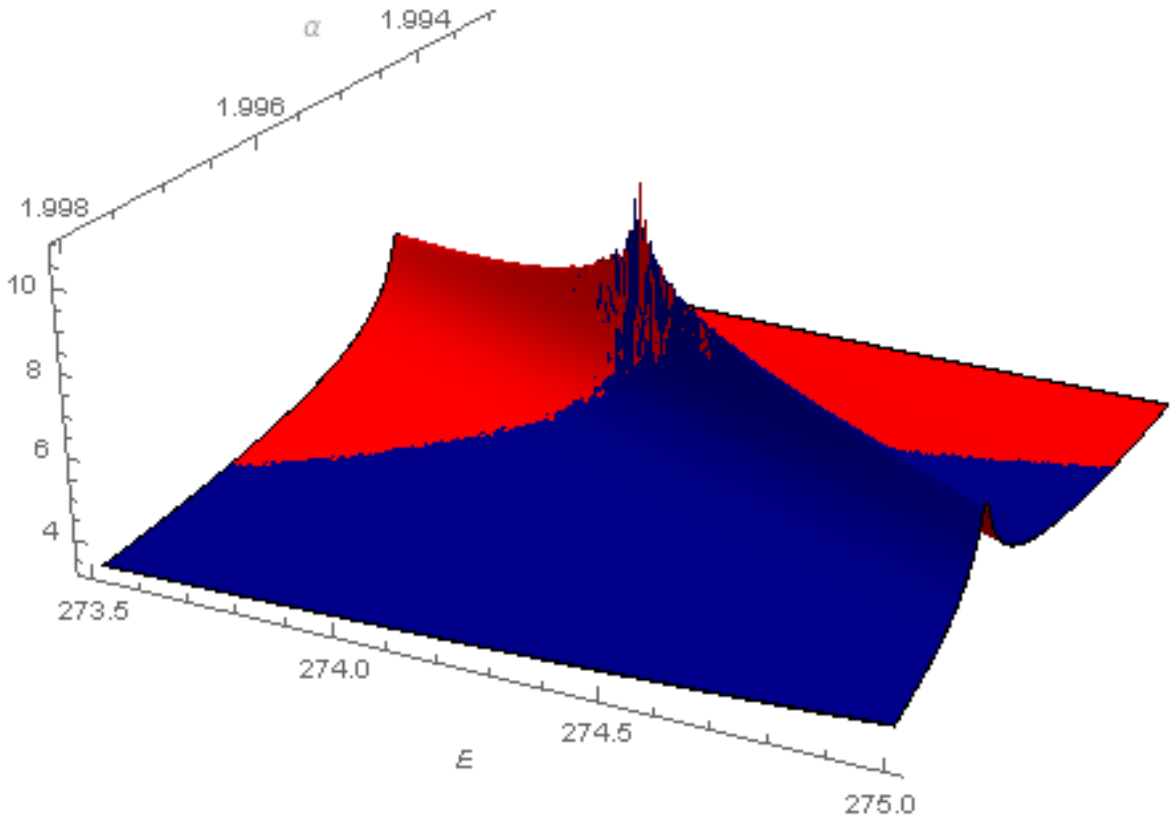

Figure: *Close view of the development of SS over $\alpha - E$ space for the first sub-peak o. Red and blue plots represent* $\log_{10} R$ *and* $\log_{10} T$ *respectively. This plot shows that in the neighbourhood of SS there are oscillations in R and T with α .*

Sub-peaks around SS for different α

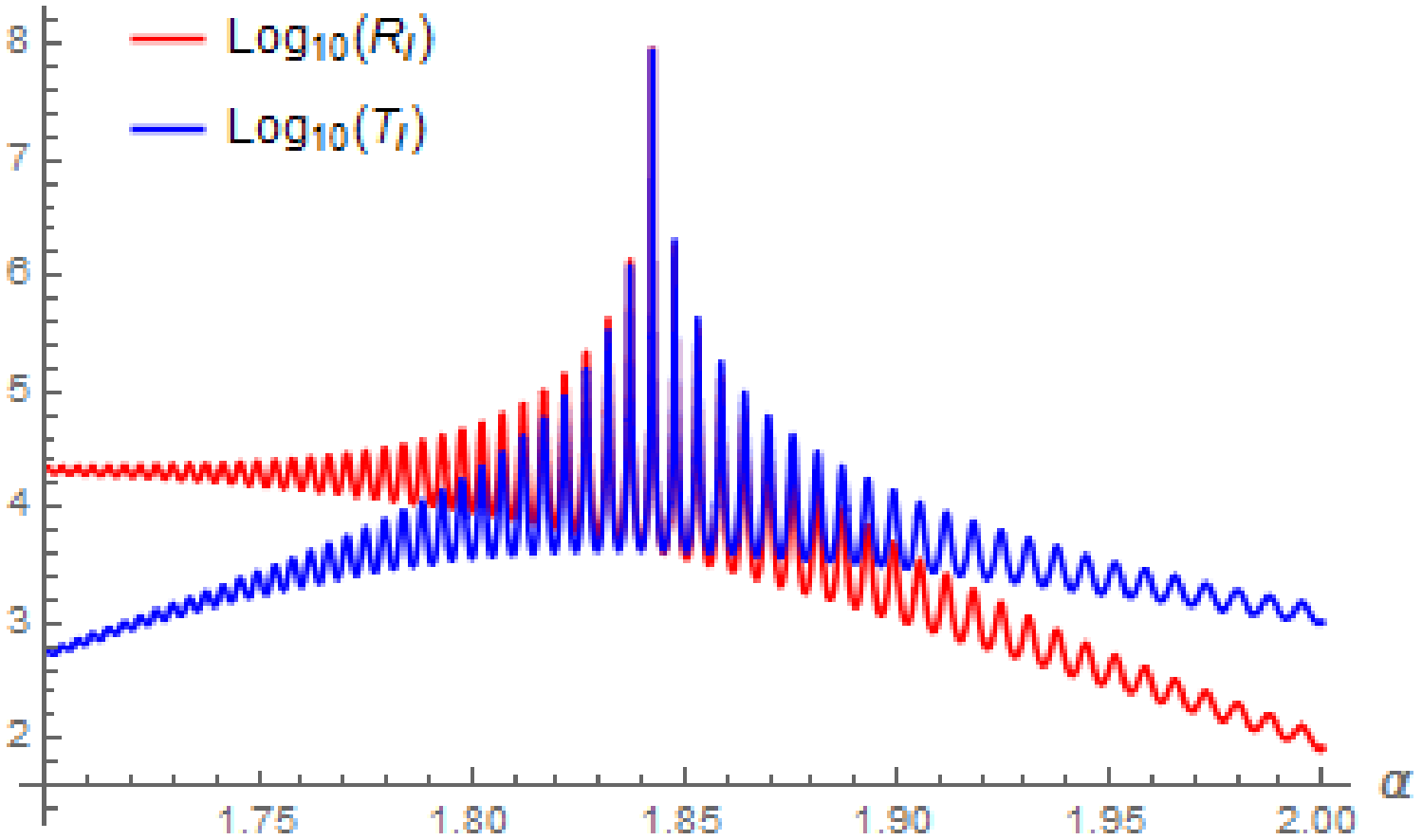

Figure: *Graphical illustrations of sub-peaks around SS with α for $E = 410$.*

CPA: Complex barrier in NHSFQM

The condition for CPA is

$$t_l t_r - r_l r_r = 0 \tag{59}$$

with $t_l = \frac{1}{m_{22}} = t_r$ and $r_l = \frac{m_{21}}{m_{22}}$, $r_r = \frac{m_{12}}{m_{22}}$. In terms of the elements of the transfer matrix, the condition is written as

$$m_{12} m_{21} = 1 \tag{60}$$

For complex barrier in SFQM this turns out

$$\mu_2^2 \sin^2 \overline{k}_\alpha b = 1 \tag{61}$$

For CPA we numerically evaluate the quantity

$$C(E, \alpha) = t_l(E, \alpha) t_r(E, \alpha) - r_l(E, \alpha) r_r(E, \alpha) \tag{62}$$

and study the variation of $\log |C|$ or $\log(\frac{1}{|C|})$ with respect to E and α for a given non-Hermitian barrier potential. We identify CPA as the deep minima in $\log |C|$ (or maxima in $\log(\frac{1}{|C|})$).

CPA: blue shifted

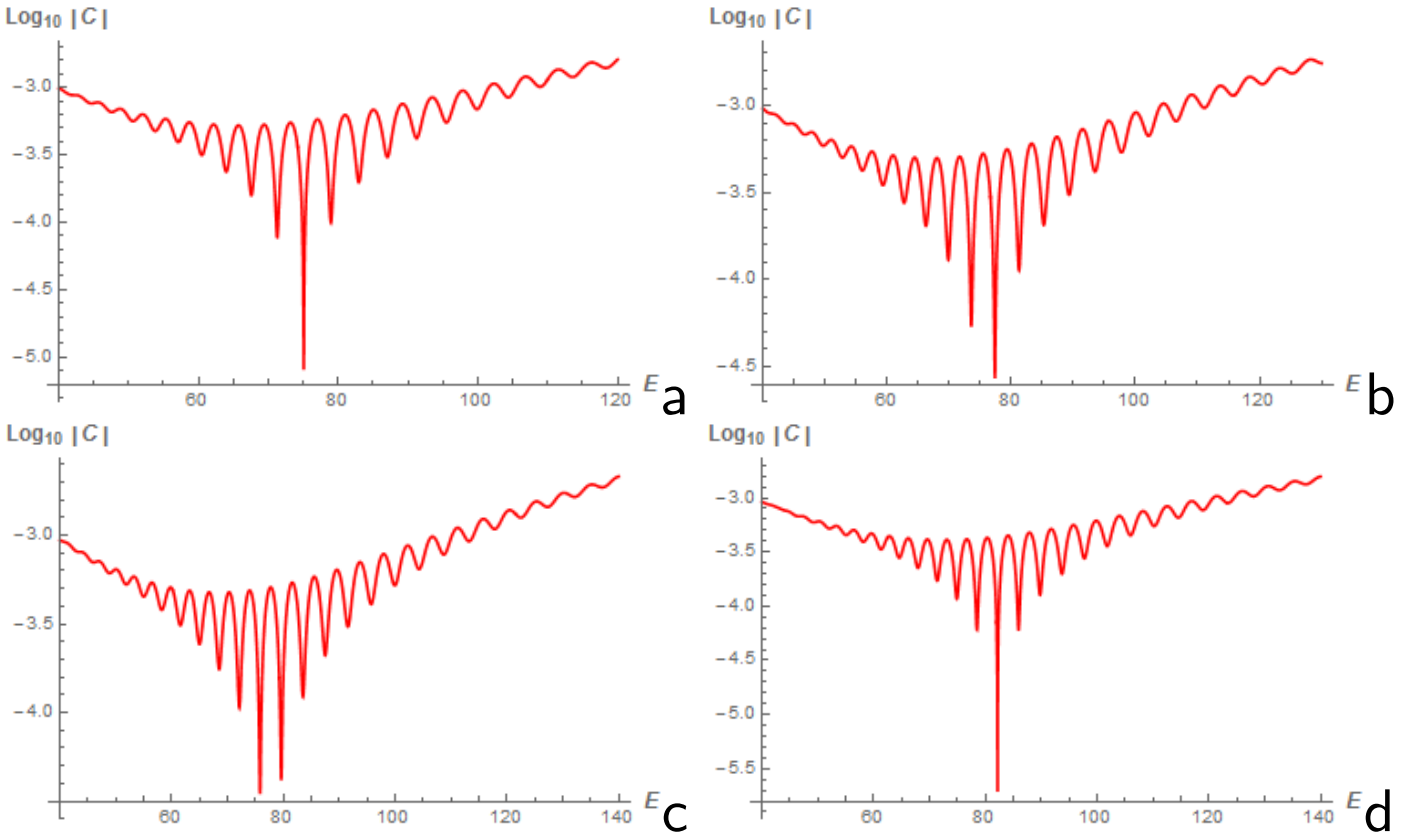

Figure: *The deep minima in* $C(E,\alpha)$ *for* $V = 0.1 + 5i$ *with* $b = 10$ *for different values of* $\alpha = 2, 1.99.1.98, 1.95$. *The CPA energy is blue shifted as* α *decreases.*

CPA: Sub-Peak

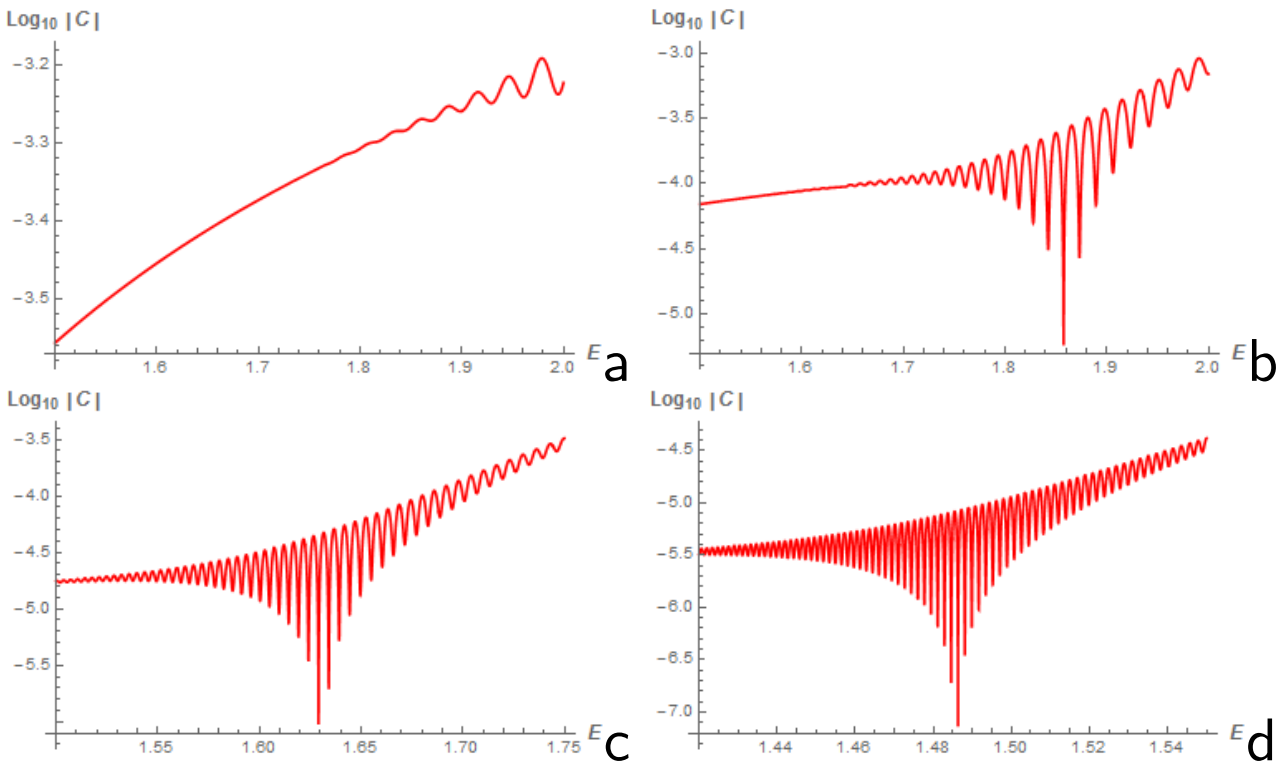

Figure: *Variation of* $\log_{10} C$ *with* α *at different energies* E *For Fig-a,b,c,d the respective energies are* $E = 50, 100, 200, 400$. *This illustrate that for higher energy, the CPA corresponds to comparatively lower* α *values. It is also observed that CPA occurring at low* α *values (and higher energies) have more dense sub-peaks with* α *in the vicinity of CPA.*

CPA: Sub-Peaks

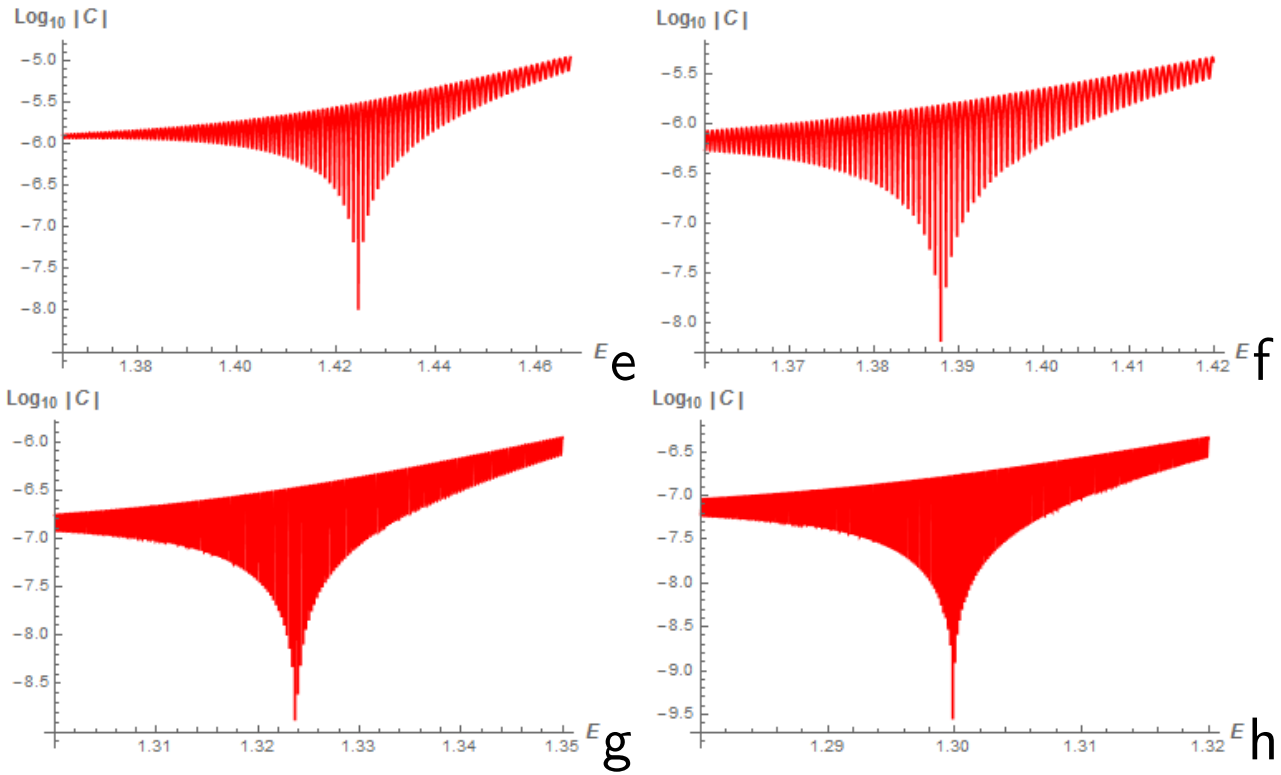

Figure: *Variation of* $\log_{10} C$ *with* α *at different energies* $E = 600, 800, 1500, 2000$. *At higher energy, the CPA corresponds to comparatively lower* α *values. CPA occurring at low* α *values (and higher energies) have more dense sub-peaks with* α *in the vicinity of CPA.*

Sub-Oscillations around CPA

- Fig , below shows the plot of $\log(|C|)$-E for different value of α for the potential $V = 0.1 + 5i$ with $b = 10$.
- Deep minima of $C(E, \alpha)$ is blue shifted with decreasing α. To understand the development of CPA, we 3D plot $\log(\frac{1}{|C|})$ with E and α.
- We see that for standard case of $\alpha = 2$, $\log \frac{1}{C}$ curve have sub-peaks (similar to the case of SS) with energy E on both side of the maxima. It is observed that the sub-peaks for $\alpha = 2$ that occur for energy $E > E^{CPA}_{\alpha=2}$ develop maxima for some value of $\alpha < 2$.

Sub-Oscillation: CPA

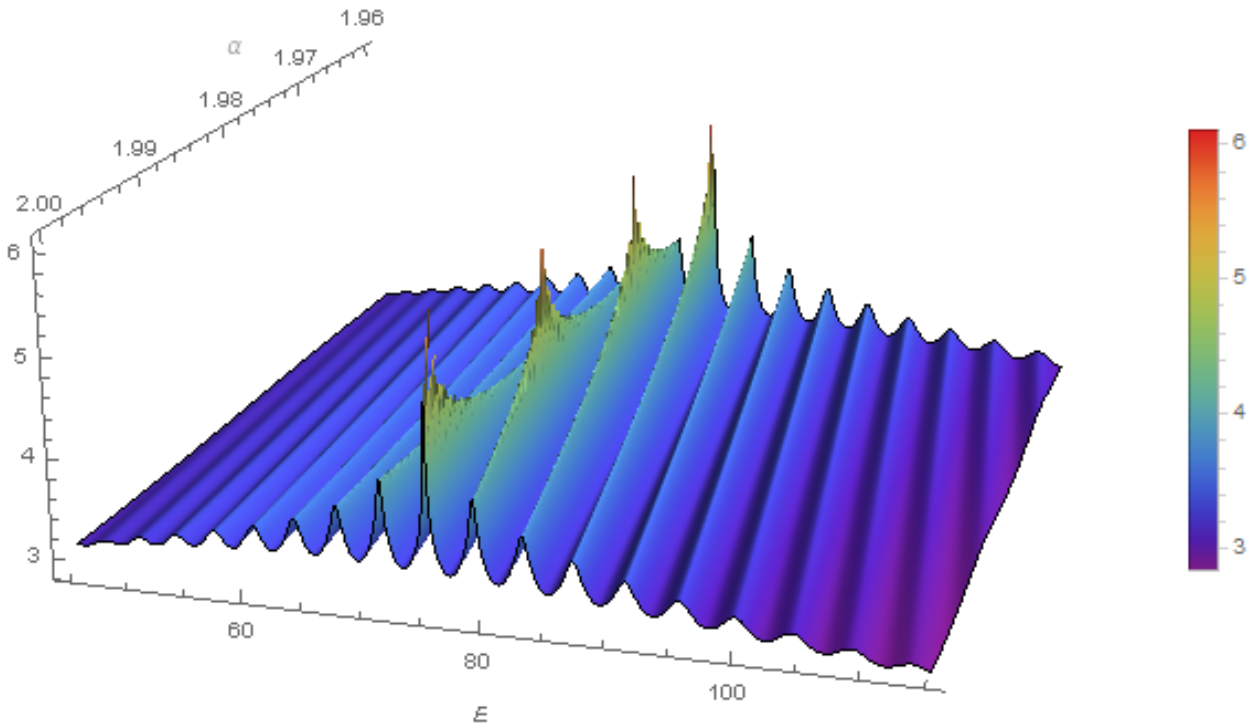

Figure: *Development of multiple CPA for $\alpha \leq 2$ over $\alpha - E$ space. the range of α is $1.96 \leq \alpha \leq 2$. The color bar is shown adjacent to the figure. It is evident that that the sub-peaks for $E > E_{CPA}^{\alpha=2}$ develop CPA for some values of $\alpha < 2$.*

More on CPA

- We have observed that the sub-peaks for $E < E_{\alpha=2}^{CPA}$ develop CPA for some values of $\alpha > 2$.
- Further similar to sub-peaks with E around the CPA, there are sub-oscillations with α in the neighbourhood of CPA . It is noticed that the CPA with lesser α values have more dense sub-minima with α around CPA.

Sub-Oscillations:CPA

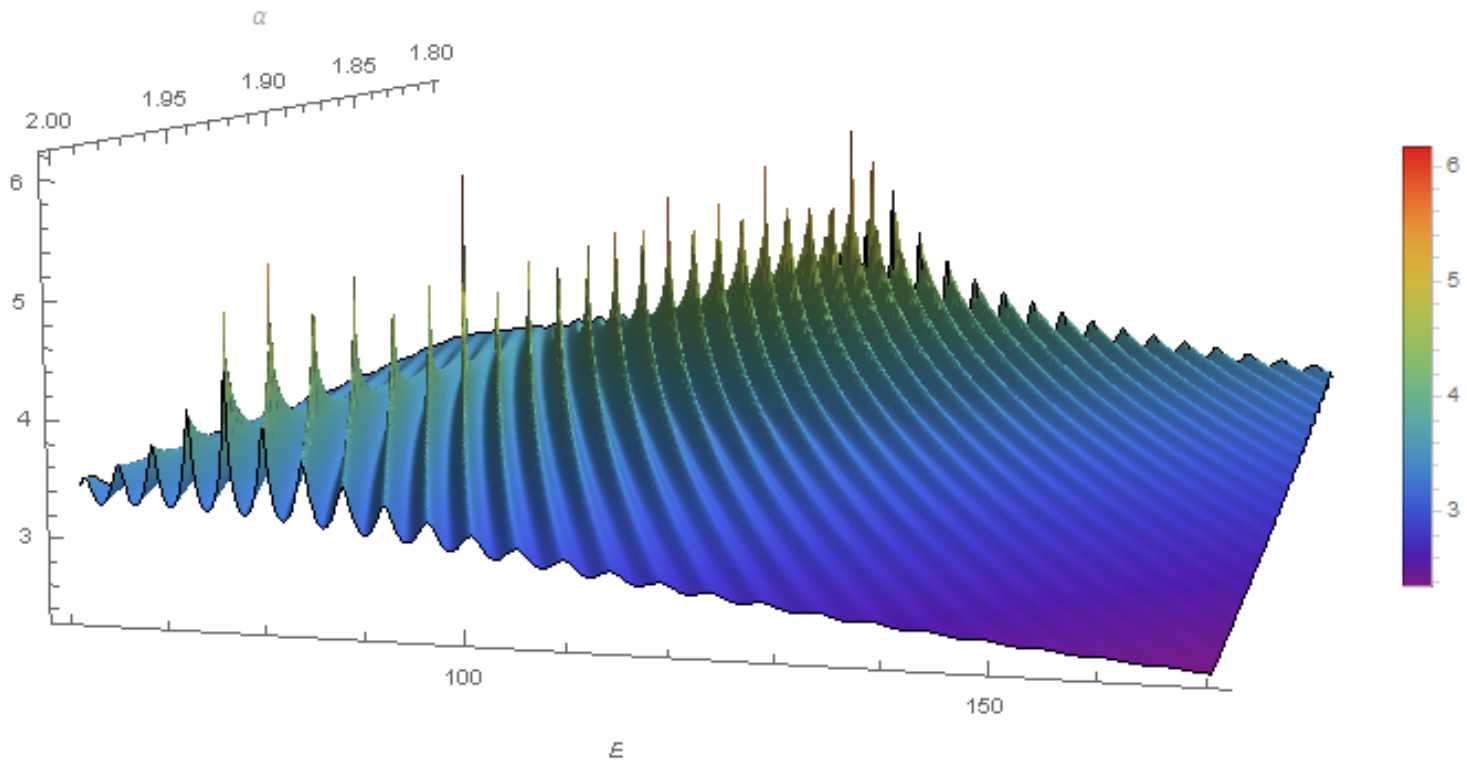

Figure: *Multiple CPA for* $1.8 \leq \alpha \leq 2$ *, over* $\alpha - E$ *space. The color bar is shown adjacent to the figure. It is evident that that the sub-peaks for* $E > E_{CPA}^{\alpha=2}$ *develop CPA for some values of* $\alpha < 2$.

Conclusions

- We consider Space fraction QM, by replacing Brownian paths by Levy flight paths.
- We discuss Hartman effect for Quantum Tunnelling by stationary phase method.
- No Hartman effect in SFQM. Tunnelling time decreases with Levy parameter α
- Result is demonstrated for one barrier but we have checked for multiple barriers.
- Hartman effect restores when Levy path $\rightarrow$ Brownian path. Hasan & Mandal PLA (2018)

Conclusions

- Non-Hermitian extension of SFQM has been considered in the context of complex delta potential and complex barrier potential.
- Scattering properties have discussed , particularly SS and CPA for both the systems.
- Non-Hermitian SFQM systems have more flexibility for SS and CPA and display some new features of scattering.
- Blue/ Red shift of SS (depending on the parameters in the potential has been observed as α decreases for both the potentials have been shown for complex δ potential.
- Blue shift has been shown for SS and CPA energy with decreasing α

Conclusions

- Possibility of multiple SS or CPA in NHSFQM. Sub Peaks converted as SS/CPA as α changes.
- It is known that the reflection and transmission amplitudes are oscillatory near the spectral singular/CPA point. It is found that these oscillations eventually develop SS/CPA in non-Hermitian SFQM.
  Hasan & Mandal, 1712.09727

Future directions

- PT symmetric Non-Hermitian extension of SFQM for consistent quantum theory.
- Tunnelling time for multiple complex barriers in SFQM, and investigation on Hartman effect. (in progress)

Thanks

Thanks of your attention.